Anti-MMP-9 Antibody: A promising therapeutic strategy for treatment of inflammatory bowel disease complications with fibrosis

Goffin, Laurence ; Fagagnini, Stefania ; Vicari, Alain ; Mamie, Céline ; Melhem, Hassan ; Weder, Bruce ; Lutz, Christian ; Lang, Silvia ; Scharl, Michael ; Rogler, Gerhard ; Chvatchko, Yolande ; Hausmann, Martin

Abstract: BACKGROUND Despite medical treatments or surgical options, more than one-third of patients with Crohn's disease suffer from recurring fistulae. Matrix metalloprotease 9 (MMP-9), a type IV collagenase that cleaves components of the extracellular matrix leading to tissue remodeling, is upregulated in crypt abscesses and around fistulae suggesting an important role for this enzyme in fistula formation. Our aims were (1) to correlate serum levels of MMP-9 degradation products in patients with CD with the presence of fistulae and (2) to investigate the impact of selective MMP-9 inhibition in a mouse model of intestinal fibrosis. METHODS Serum MMP-9 degradation products were quantified in subjects affected with nonstricturing and nonpenetrating CD (n = 50), stricturing CD (n = 41), penetrating CD (n = 22), CD with perianal fistula (n = 29), and healthy controls (n = 10). Therapeutic efficacy of anti-MMP-9 monoclonal antibodies was assessed in a heterotopic xenograft model of intestinal fibrosis. RESULTS C3M, an MMP-9 degradation product of collagen III, demonstrated the highest serum levels in patients with penetrating CD and differentiated penetrating CD from other CD subgroups and healthy controls, P = 0.0005. Anti-MMP-9 treatments reduced collagen deposition and hydroxyproline content in day-14 intestinal grafts indicating reduced fibrosis. CONCLUSIONS The serologic biomarker C3M can discriminate penetrating CD from other CD subgroups and could serve as marker for the development of penetrating CD. Anti-MMP-9 antibody has therapeutic potential to prevent intestinal fibrosis in CD complications.

DOI: https://doi.org/10.1097/MIB.0000000000000863

Anti-MMP-9 Antibody: A Promising Therapeutic Strategy for Treatment of Inflammatory Bowel Disease Complications with Fibrosis

Laurence Goffin, PhD, Stefania Fagagnini, MD,† Alain Vicari, DVM, PhD,* Céline Mamie,† Hassan Melhem, PhD,† Bruce Weder, MSc ETH Pharm Sc,† Christian Lutz, MD,† Silvia Lang,† Michael Scharl, MD,† Gerhard Rogler, MD, PhD,† Yolande Chvatchko, PhD,* and Martin Hausmann, PhD†*

Background: Despite medical treatments or surgical options, more than one-third of patients with Crohn's disease suffer from recurring fistulae. Matrix metalloprotease 9 (MMP-9), a type IV collagenase that cleaves components of the extracellular matrix leading to tissue remodeling, is upregulated in crypt abscesses and around fistulae suggesting an important role for this enzyme in fistula formation. Our aims were (1) to correlate serum levels of MMP-9 degradation products in patients with CD with the presence of fistulae and (2) to investigate the impact of selective MMP-9 inhibition in a mouse model of intestinal fibrosis.

Methods: Serum MMP-9 degradation products were quantified in subjects affected with nonstricturing and nonpenetrating CD (n = 50), stricturing CD (n = 41), penetrating CD (n = 22), CD with perianal fistula (n = 29), and healthy controls (n = 10). Therapeutic efficacy of anti-MMP-9 monoclonal antibodies was assessed in a heterotopic xenograft model of intestinal fibrosis.

Results: C3M, an MMP-9 degradation product of collagen III, demonstrated the highest serum levels in patients with penetrating CD and differentiated penetrating CD from other CD subgroups and healthy controls, $P = 0.0005$. Anti-MMP-9 treatments reduced collagen deposition and hydroxyproline content in day-14 intestinal grafts indicating reduced fibrosis.

Conclusions: The serologic biomarker C3M can discriminate penetrating CD from other CD subgroups and could serve as marker for the development of penetrating CD. Anti-MMP-9 antibody has therapeutic potential to prevent intestinal fibrosis in CD complications.

(Inflamm Bowel Dis 2016;22:2041–2057)

Key Words: fibrosis, anti-MMP-9-antibody, mouse, transplantation, collagen

Crohn's disease (CD) is a chronic immune-mediated inflammatory condition of the gastrointestinal tract. Initially, the majority of patients develop a purely inflammatory presentation of disease (Montreal Class B1 inflammatory phenotype). However, some patients eventually develop intestinal fibrosis leading to the development of severe complications, such as intestinal strictures (Montreal Class B2 fibrostenotic phenotype) and fistulae (Montreal B3 penetrating phenotype).[1,2] The development of fistulae in the course of the disease is a common complication. Fistula formation has been reported in 17% to 50% of patients with CD in population-based studies and about 35% of patients with CD suffer from at least one fistula during the course of their disease.[3] A fistula is an abnormal channel or passageway connecting 2 parts of the bowel or the bowel to the vagina, bladder, or skin. The occurrence of fistulae results in considerable morbidity, including permanent sphincter and perianal tissue destruction as well as professional and personal disabilities. Despite current medical options, including antibiotics, immunosuppressants (such as azathioprine or cyclosporine), anti-TNF antibodies and surgery, permanent closure of fistula can only be achieved in about one-third of patients with CD[4] and a further third suffer from recurring fistulae,[5] indicating that new and more effective therapeutic approaches are urgently needed for patients suffering from CD-associated fistulae. CD-associated fistulae originate from an epithelial defect that may be caused by ongoing inflammation. Having undergone epithelial-to-mesenchymal transition (EMT), intestinal epithelial cells penetrate into deeper layers of the mucosa and the gut wall, causing localized tissue damage and formation of a tube-like structure that connects the gastrointestinal

Supplemental digital content is available for this article. Direct URL citations appear in the printed text and are provided in the HTML and PDF versions of this article on the journal's Web site (www.ibdjournal.org).

Received for publication April 21, 2016; Accepted May 5, 2016.

From the *Calypso Biotech SA, Plan-les-Ouates, Geneva, Switzerland; and †Clinic of Gastroenterology and Hepatology, Department of Internal Medicine, University Hospital Zurich, Zurich, Switzerland.

Supported by a grant from the Swiss Commission for Technology and Innovation (KTI 16405.1 PFLS-LS).

G. Rogler discloses grant support from AbbVie, Ardeypharm, MSD, FALK, Flamentera, Novartis, Roche, Tillots, UCB, and Zeller. The remaining authors have no conflict of interest to disclose.

L. Goffin and S. Fagagnini are equal contributors.

Reprints: Martin Hausmann, PhD, Division of Gastroenterology and Hepatology, University Hospital Zürich, University of Zurich, 8091 Zurich, CH-Switzerland (e-mail: martin.hausmann@usz.ch).

DOI 10.1097/MIB.0000000000000863

Published online 10 August 2016.

tract to other organs or the skin. EMT enhances the activation of matrix remodeling enzymes, such as matrix metalloproteinases MMP-3 and MMP-9, causing further tissue damage and inflammation.[6,7] MMP-9 (also known as gelatinase B) is a zinc-dependent endopeptidase responsible for the degradation of gelatin, denatured collagens, and basement membrane.[8] It is involved in many developmental processes, including angiogenesis, wound healing, and extracellular matrix (ECM) degradation. Additional roles for MMP-9 have recently emerged, including its ability to regulate cell migration, invasion, cell signaling, and EMT in multiple tissues.[9–11] MMP-9 is the most abundantly expressed protease in inflamed CD tissues, and its upregulation leads to an increase in net MMP proteolytic activity.[12–14] In biopsies from CD mucosa, MMP-9 was found as monomers and oligomers, as latent (pro-) and mature forms, and complexed with other molecules. Pro-MMP-9 and MMP-9 complexed to TIMP-1 are inactive, whereas MMP-9 associated with neutrophil gelatinase–associated lipocalin (NGAL) is enzymatically active.[15] Both inactive and active MMP-9 are expressed surrounding CD fistulae. Moreover, increased mRNA and protein levels, of MMP-9 and of its physiological activator MMP-3, were found in granulocytes, mononuclear cells, and fibroblasts,[13] suggesting an important role for these enzymes in fistula formation.

Serum and urinary levels of MMP-9 correlate with disease activity in CD and ulcerative colitis (UC).[16,17] MMP-3 and MMP-9 serum levels were suggested to be useful markers of disease activity in children with UC[18] and in inflammatory bowel disease (IBD).[19] Circulating levels of NGAL or the NGAL/MMP-9 complex have recently been described as a potential biomarker for mucosal healing in UC treated with infliximab, with reduced serum levels being predictive of mucosal healing.[20,21] These fluctuating circulating levels of MMP-9 reflect the changes of MMP-9 concentration in the organ, but not of its activity. Therefore, a method allowing the quantification of MMP-9 activity in serum mirroring its activity in tissue would aid in the diagnosis, in the monitoring of the course of disease, and in the evaluation of the effectiveness of IBD treatment.

The involvement of MMPs for the development of CD is highlighted by the fact that in the mouse dextran sodium sulfate (DSS)-induced colitis model, targeted deletion of *Mmp9* has a protective effect,[22,23] whereas mice overexpressing MMP-9 in the intestinal epithelium develop more severe colitis when compared with wild-type animals.[24] At present, no animal model that reproduces the unique histological features associated with CD intestinal fistulae exists, but there are several models that address specific aspects of the pathogenesis of CD fistulae. One of these, the heterotopic transplant mouse model developed recently could be used to investigate intestinal fibrosis.[25]

In this study, we show that, in patients with penetrating CD, increased MMP-9 expression associated with fistula tracks is reflected by elevated serum levels of C3M, an MMP-9 degradation type III collagen product. We also report the efficacy of 2 independent selective anti-MMP-9 monoclonal antibodies in the heterotopic transplant mouse model of intestinal fibrosis. Collectively, these data indicate that MMP-9 plays a key role in the modulation of intestinal fibrosis and suggest that selective MMP-9 inhibition is a promising therapeutic strategy for the treatment of penetrating CD.

MATERIALS AND METHODS

Tissue and Serum Samples from Patients with IBD and Healthy Controls

Perianal fistula specimens from patients were prospectively collected for immunohistochemistry (IHC) from men and women with and without CD. We investigated 5 fistulae in formalin-fixed tissue samples from 5 patients with perianal fistulae as indicated in Table 1. Tissue samples were surgically resected and immediately transferred to 4% formalin and stored at 4°C until further analysis. Written informed consent was obtained before specimen collection, and the studies were approved by the local ethics committee.

Ethical Considerations

The experimental protocol for animals was approved by the local Animal Care Committee of the University of Zurich (registration number ZH183/2014).

Written informed consent was obtained before human specimen collection and studies were approved by the local ethics committee. The cohort study is supported by the Swiss National Science Foundation and approved by the local ethical committees (IRB approval number: EK-1316, approved

TABLE 1. Characteristics of Patients with Perianal Fistulae

Patients	F20	F21	F22	F23	F24
Comment	Secondary fistula	Secondary fistula, drainage	Gluteal fistula system	Intersphincteric fistula	Fistula with abscess
Gender	Female	Male	Male	Male	Female
Age (yrs) at time of sampling	25	72	59	41	46
Fistula since, yrs	1–3	<1	>3	<1	<1
Diagnosis	CD	non-CD	CD	non-CD	non-CD
Medication	Yes	No	No	No	No

on February 5, 2007 by the Cantonal Ethics Committee of the Canton Zürich, Switzerland).

Serum samples were obtained from HC between 29 and 49 years of age, with no history of IBD or treatment for such disease. All subjects felt healthy and had no reported pain or symptoms of any disease, and all gave their written informed consent. Serum samples from patients suffering from CD were obtained from the Swiss Inflammatory Bowel Disease Cohort Study. All patients had an established diagnosis of CD.[26] Patients had received standard care, including physical therapy, and treatment with antibiotics, 5-aminosalicylates, corticosteroids, azathioprine, 6-mercaptopurine, methotrexate, cyclosporine, and/or TNF inhibitors such as infliximab (Remicade; Centocor), adalimumab (Humira; AbbVie), and certolizumab pegol (Cimzia; UCB). Patients were classified into subgroups according to the Montreal classification,[2] as indicated in Table 2.

Biomarker Assays

Several neoepitope fragments resulting from ECM synthesis and degradation were assessed by solid phase competitive enzyme linked immunosorbent assays (ELISAs) developed by Nordic Bioscience Laboratory. A selection of 5 MMP-9-specific degradation products from collagen and ECM proteins were quantified in serum samples from healthy controls (HC) and from patients with penetrating CD (group B3 of CD), using competitive ELISAs. The C3M ELISA measures type III collagen fragments[27] and the BGM ELISA measures biglycan fragments, both generated by MMP-9 in connective tissues.[28] The C1M ELISA measures type I collagen fragments generated by MMP-2, MMP-9, and MMP-13 in connective tissues.[29] The C6M ELISA measures type VI collagen fragments generated by MMP-2 and MMP-9 in muscles[30,31] and the LAM ELISA measures laminin fragments generated by MMP-2 and MMP-9 in basement membranes. C3M fragment was measured in serum samples from HC and from all groups of patients with CD.

Anti-MMP-9 Antibody Production

Anti-MMP-9 binders have been isolated using single-chain fragment variable (scFv) phage display selection and screening technology. The Dübel HAL7 (Lambda) scFv library was obtained from the Mab Factory company (Braunschweig, Germany). The selection of phages that bind the target was performed using biotinylated recombinant human or mouse MMP-9 proteins, immobilized on streptavidin paramagnetic beads. These recombinant

TABLE 2. Characteristics of Patients with CD and of HC

Baseline Characteristics	CD B1 (Nonstricturing and Nonpenetrating CD) (n = 50)	CD B2 (Stricturing CD) (n = 41)	CD B3 (Penetrating CD) (n = 22)	CD B3p (CD with Perianal Fistula) (n = 29)	HC (n = 10)
Gender					
Female, (%)	22 (44)	25 (61)	8 (36)	19 (65)	6 (60)
Male, (%)	28 (56)	16 (39)	14 (64)	10 (35)	4 (40)
Age, mean years (range)	40.36 (17–71)	47.51 (23–79)	36.55 (16–63)	39.43 (22–64)	37.67 (29–49)
Duration of disease at sampling, median year, (range)	8 (0–34)	15 (0–35)	13 (1–37)	8 (2–38)	NA
Clinical disease activity at sampling					
Active, (%)	17 (34)	12 (30)	8 (36)	9 (31)	NA
Quiescent, (%)	33 (66)	29 (70)	14 (64)	20 (69)	NA
Abscess at time of sampling	0	0	15	2	NA
Stenosis at the time of sampling	0	29	11	7	NA
History of intestinal surgery	16	34	15	9	NA
Medication					
5-aminosalicylates	12	12	7		NA
Steroid	11	14		8	NA
Azathioprine/6 mercaptopurine	18	22	5	7	NA
Methotrexate	5	1		3	NA
Anti-TNFα	13	11	5	10	NA
Antibiotics	1	3		2	NA
Cyclosporine			2		NA
Immunosuppressor + anti-TNFα (Combo therapy)			9		NA

proteins were generated by cloning the full-length cDNA of human (NM_004994) or mouse (NM_013599) *Mmp9* into the pBluescript II vector and by transiently transfecting it into HEK-293 cells (ATCC, Molsheim, France). Binders to MMP-9 proteins (and not to MMP-2) were then screened for neutralizing activity in a cell-free enzymatic activity assay, using either full-length MMP-9 or MMP-9 catalytic domain and a fluorogenic substrate (porcine DQ-Gelatin from Invitrogen, Ref D12054). Optimization of selected hit candidates was performed, by affinity maturation conducted through lambda light chain shuffling followed by germlining and by CDR mutations. After these optimization steps, the fully human anti-human MMP-9 antibody CALY-001 was selected and expressed as human IgG4/kappa antibody in transiently transfected Chinese hamster ovary cells. A comparator antibody, the AB0046-h4 mouse monoclonal antibody against mouse MMP-9, was generated using sequences of the variable regions of AB0046 antibody described in patent WO2012/027721A2. AB-0046 is a selective and potent allosteric antibody inhibitor of mouse MMP-9, which was shown to reduce disease severity in a DSS-induced mouse model of UC.[32] The construct was subcloned and expressed as human IgG4/kappa antibody in transiently transfected CHO cells. Antibodies were purified using Protein A agarose, MAbSelect SURE (Sigma Aldrich, Ref 17-5438-01) and resuspended in phosphate-buffered saline, pH 7.4. Production batches exhibit protein purity, estimated by SDS-PAGE resolution, greater than 95% and endotoxin levels, quantified by a commercial kit, lower than 1 EU/mL.

MMP-9 Enzymatic Assays

Gelatinase activity of natural forms of MMP-9 was assessed using a cell-free enzymatic assay. Briefly, a flat bottom nonbinding 96-well black plate was filled with monomeric, dimeric, or NGAL-bound form of MMP-9 purified from human neutrophils (0.24 ng/μL final) and with the catalytic domain of recombinant human MMP-3 (Calbiochem, Ref 444217, 0.90 ng/μL final). After an overnight activation at RT, serial dilutions of CALY-001 and anti-MMP-9 antibody were added and incubated for 1 hour at RT. The enzymatic reaction was initiated by addition of the porcine fluorogenic substrate DQ-Gelatin, and the incubation was performed at RT in the dark for 2 hours. The intensity of the fluorometric reaction was measured by reading light emission at 520 nm on excitation at 485 nm (Ex485/Em520). The resulting fluorescence values are proportional to the remaining enzymatic activity in each well. Data were corrected by withdrawal of their respective negative (no enzyme) control wells and plotted against antibody concentrations. A 4-parameter curve fit was used with Prism software (GraphPad, v6.0) to determine the half maximal inhibitory concentration (IC_{50}) of the CALY-001 antibody against each MMP-9 species tested.

For testing the selectivity of the CALY-001 antibody for MMP-9 versus other MMP enzymes, a commercial kit (MMP Inhibitor profiling kit, Enzo, Ref BML-AK308) was used following the manufacturer's instructions. Briefly, a flat bottom nonbinding 96-well black plate was filled with the catalytic domain of each human MMP available in the kit. An optimal dilution of CALY-001 antibody (100 nM final) was then added and incubated for 1 hour at RT. A control reaction, replacing CALY-001 antibody by the small molecule MMP inhibitor N-Isobutyl-N-(4-methoxy-phenyl sulfonyl) glycyl hydroxamic acid (NNGH, 1.3 μM final), was also included in the study. Enzymatic activity was revealed on the addition of OmniMMP RED substrate (Enzo, Ref BML-P277-0100) and measured by reading light emission at 590 nm on excitation at 540 nm (Ex540/Em590). The resulting fluorescent values are proportional to the remaining enzymatic activity in each well. Results are expressed as mean percentages of remaining activity (%), with 100% set for reaction without antibody.

The kinetics and affinity of antibody binding to MMP-9 were determined by surface plasmon resonance using a BIAcore T200. Briefly, antibodies were captured onto anti-human Fc-coated surface and the target protein, pro-MMP-9 or MMP-3-activated MMP-9, was dose-titrated from 4.7 to 150 nM in a 2-fold step dilution. Analysis of the resulting sensograms provides values of apparent dissociation constant (K_D).

Heterotopic Intestinal Transplant Model

Female B6-Tg(UBC-GFP)30Scha/J donor mice (GFP-Tg)[33] weighing 20 g were bred at the University of Zurich. Female 10-week-old C57BL/6J-Crl1 mice (C57BL/6) were obtained from Charles River. The animals received standard laboratory mouse food and water ad libitum. They were housed under specific pathogen-free conditions in individually ventilated cages. The experimental protocol was approved by the local Animal Care Committee of the University of Zurich (registration number ZH183/2014).

The heterotopic mouse intestinal transplant model has been described in detail.[25] In short, donor small bowel resections were extracted and transplanted subcutaneously into the neck of recipient animals. All procedures were performed using a sterile nontouch technique. Donor mice were euthanized and after an initial anterior midline incision, the abdomen was opened completely to avoid contamination of the inner organs with hair. The small bowel was then exposed and carefully unfolded by cutting mesentery where necessary. From the small bowel proximal to the caecum a segment of 6 cm was excised. The resection was then flushed with 5 mL of 0.9% NaCl to remove stool and divided into 6 equal 10-mm parts. Resections were kept moist with 0.9% NaCl solution, whereas the recipient animals were prepared for transplantation. Recipient animals were anesthetized with isoflurane and ocular lubricant was applied (Vitamin A Blache Augensalbe 5 g, Ref 109778). A small area of the back was shaved to avoid contamination with hair. Two subcutaneous pouches were prepared through a small incision perpendicular to the body axis on either side of the neck. A small bowel resection was implanted into each of the subcutaneous pockets, and the skin was closed using vicryl 5-0 stiches or a 3M Precise Vista skin stapler. A single dose of cefazolin (Kefzol, 1g diluted in 2.5 mL distilled water; Teva Pharma AG, Basel, Switzerland) was applied intraperitoneally as prophylaxis against infection.

Monoclonal anti-MMP-9 antibodies (CALY-001 and AB-0046-h4) and the isotype control antibody were administered

intraperitoneally at 30 mg/kg on day 5, 8, and 11 after transplantation. At study termination 14 days after transplantation, recipient mice were euthanized and intestinal grafts were explanted. Each explanted graft was divided into 3 equal segments. One segment was fixed in 4% formalin and prepared for histopathological assessment. The other segments were snap frozen in liquid nitrogen and stored at −80°C until RNA and protein extractions were performed. The sections were examined with the Imager Z2 microscope (Zeiss) and the software AxioVision (Zeiss). Sirius Red stained slides were analyzed under bright field using a polarization filter. Under polarized light Sirius Red–stained collagen assumes a palette of colors ranging from green to red as a sign for increasing maturation of the fibrotic process. Collagen layer thickness was measured by an investigator blinded to study groups. Means of collagen layer thickness were calculated from at least 8 places in representative areas at 10-fold magnification.

IHC and Immunofluorescence

For the detection of MMP-9 by IHC, heat-mediated antigen retrieval was performed using Tris-HCl/EDTA buffer pH 9 (Ventana, Ref 950224). MMP-9 was stained with a rabbit monoclonal antibody from Abcam (Ref ab137867, dilution 1:800). An HRP-polymer conjugated anti-rabbit IgG was used as secondary antibody. EnVision HRP stain system (labeled polymer anti-rabbit, Dako) was used for visualization. All sections were counterstained with hematoxylin.

For the detection of human IgGs by IHC, protease 1 pretreatment was performed (Ventana, 12 minute). Human IgGs were stained with a polyclonal rabbit anti-human antibody from Dako (Ref A0423, dilution 1:15,000). Ultra Map anti-rabbit antibody (Ventana) was used as secondary antibody (immunstainer, Ventana Discovery Ultra Stainer). ChromoMap DAB kit (Ventana) was used for visualization. IHC of sections isolated from human tonsil was the positive control, and IHC in the absence of primary antibody of sections from freshly isolated small bowel was the negative control.

For the detection of E-cadherin or α-smooth muscle actin (SMA) by immunofluorescence (IF), heat-mediated antigen retrieval was performed using either citrate buffer pH 9.0 (Dako, Ref S2367) or citrate buffer pH 6.0 (Dako, Ref S1699), respectively. E-cadherin was tagged with a rabbit monoclonal antibody from Cell Signaling (Ref 3195, dilution 1:200). Alpha-SMA was tagged with a rabbit polyclonal antibody from Abcam (Ref ab5694, dilution 1:200). An Alexa Fluor 647 dye-coupled anti-rabbit IgG (Life Technologies, Ref A21244) was used as secondary antibody. All sections were counterstained with 4′,6-diamidino-2-phenylindole (DAPI). The sections were examined with the Imager TCS SP5 (Leica) and the software LAS AF (Leica).

Zymography

The activity of MMP-9 was measured by zymography in homogenates of intestinal grafts as previously described.[34] Briefly, intestinal grafts were homogenized on ice in lysis buffer (25 mM Tris-HCl pH 7.5, 100 mM NaCl, and 1% IGEPAL), containing protease inhibitors (10 μg/mL aprotinin, 2 μg/mL leupetin, 4 mM benzamidine), using disposable pellet Pestles (Sigma, Ref Z359947). The total protein concentration of the resulting homogenates was determined by Bradford assay. Equivalent protein amounts (10 μg) of each homogenate were mixed with electrophoresis loading buffer x2 (1:1; vol:vol) and resolved by zymography using Novex 10% Zymogram Protein Gels (Ref EC61752BOX), as described in the manufacturer's instructions. The gelatinase activities appear as transparent bands against the background of Coomassie brilliant blue-stained gelatin. Pro-MMP-9 and MMP-9 species were identified by comparison of their migration to that of purified pro-MMP-9 and MMP-9 recombinant proteins. Pictures of zymogram gels were acquired using the Azure C200 gel imaging system and semiquantitative analysis of total MMP-9 amounts was performed using ImageJ software (version 1.49). Results are expressed as arbitrary units.

Hydroxyproline Determination

Hydroxyproline content was quantitated from freshly isolated small bowel and grafts using the chloramine T colorimetric method[35] with minor modifications.[36] In brief, tissues (20–50 mg) were weighed and hydrolyzed in 500 μL of 6 N HCl at 100°C for 24 hours. The hydrolysate was filtered using a 0.2 μm syringe filter. Samples (20–50 μL) were dried in a vacuum evaporator. Dried samples were incubated with 500 μL of chloramine T solution (1 part 7% chloramine T and 4 parts citrate/acetate buffer [pH 6.0, 695 mM sodium acetate, 128 mM trisodium citrate_$2H_2O$, 29 mM citric acid, and 38.5% isopropanol]) at room temperature for 25 minutes. Five hundred microliter of Ehrlich's solution (1.4 M dimethylaminobenzaldehyde, 20% perchloric acid and 67% isopropanol) was then added, and samples were incubated at 65°C for 20 minutes for chromophore formation. After cooling, the absorbance was read at 561 nm. Hydroxyproline concentration was calculated from a standard curve prepared with high-purity hydroxyproline. The results were expressed as micrograms of hydroxyproline per gram of tissue.

ELISA for MMP-9 Activity Assay in Serum

Quantification of MMP-9 activity in homogenates of intestinal grafts was performed by ELISA, using the mouse MMP-9 activity assay kit from QuickZyme (Ref QZBMMP9m). Briefly, equivalent amounts of total proteins of each graft homogenate were dispensed onto 96-well plate, precoated with anti-mMMP9 antibody. After overnight incubation at 4°C, wells were washed with phosphate-buffered saline/0.05% Tween 20, and the detection reagent (peptide substrate of MMP-9) provided in the kit was added to quantify active mature MMP-9. Release of chromogenic cleaved peptide was measured at 405 nm using an ELISA plate reader. A calibration curve derived from results obtained with known amounts of mouse MMP-9 standards was used to determine amounts of active MMP-9 in tested samples. The lower limit of quantification of this assay is 1 pg/mL.

ELISA for TGFβ Protein Quantification

Quantification of TGFβ in homogenates of intestinal grafts was performed by ELISA, using the mouse TGF-β1 Duoset kit (R&D Systems, Ref DY1679). The protocol is similar to that used for monitoring of MMP-9 activity, with direct reading of total TGFβ and specific reading of active TGFβ species after the acidic activation of the samples. The quantification range of this assay is 31.2 to 2000 pg/mL.

TaqMan Gene Expression Assays

Genes and names of the probes used to quantify their expression are the followings: *Mmp9*; Mm00442991_m1, *Timp1*; Mm00441818_m1, transforming growth factor beta 1 (*Tgfb1*); Mm01178820_m1 and *Gapdh*; 4352339E. The relative cDNA concentration for the genes of interest was calculated using the ddCt-method.

Statistical Analysis

Data were analyzed and visualized using Prism software (GraphPad, v6.0). Statistical analysis was performed using one-way analysis of variance with Dunnett's Multiple Comparison posttest or unpaired t test with Welch's correction for pairwise analysis. Statistical analysis for quantification of gene expression and MMP-9 activity levels was assessed by Kruskal–Wallis analysis.

RESULTS

MMP-9 is Strongly Expressed in Tissue Alongside Fistula Tracts

Histological analysis of colonic tissue specimens showed a strong staining for MMP-9 in the tissue surrounding the fistula tracts of patients with perianal fistulae (Fig. 1A, B). Staining was most prominent in squamous cell epithelia associated with the distal part of the fistula tract. Marked staining in the distal part was clearly defined to an unstained proximal part. In addition, we found MMP-9 staining in epithelial cells of deformed crypts directly next to the fistula tracts (Fig. 1C) and in inflammatory, mainly lymphocytic, infiltrates adjacent to the fistula tracts (Fig. 1D) compared with a weaker staining at sites distant from fistula. These findings demonstrate that MMP-9 is expressed in squamous cell layers, epithelial cells of deformed crypts alongside and next to fistulae, as well as in inflammatory infiltrates, suggesting an involvement of MMP-9 in the pathogenesis of colon fistulae.

C3M, an MMP-9-generated Fragment of Type III Collagen, is a Potential Biomarker of Penetrating CD

We hypothesized that the elevated MMP-9 expression observed in intestinal biopsies from patients with CD with fistula (penetrating CD, B3 group) was associated with increased local MMP-9 enzymatic activity, leading to the release of MMP-9-generated protein-degradation products, locally and into the circulation. To investigate whether certain MMP-9-generated protein fragments could be biomarkers of penetrating CD, and/or subgroups of patients with CD, we selected 5 peptides released either by MMP-9 (C3M and BGM), MMP-2/9 (C6M and LAM), or MMP-2/9/13 (C1M), mediated proteolysis, and compared their levels in serum from B3 patients to those in serum from HC. Characteristics of these subjects are reported in Table 2. C3M (MMP-9-generated type III collagen fragment) was the only neo-peptide that demonstrated significant difference between the 2 groups, with a 1.9-fold serum level increase in CD B3 patients compared with levels observed in HC ($P = 0.0005$, Table 3). In

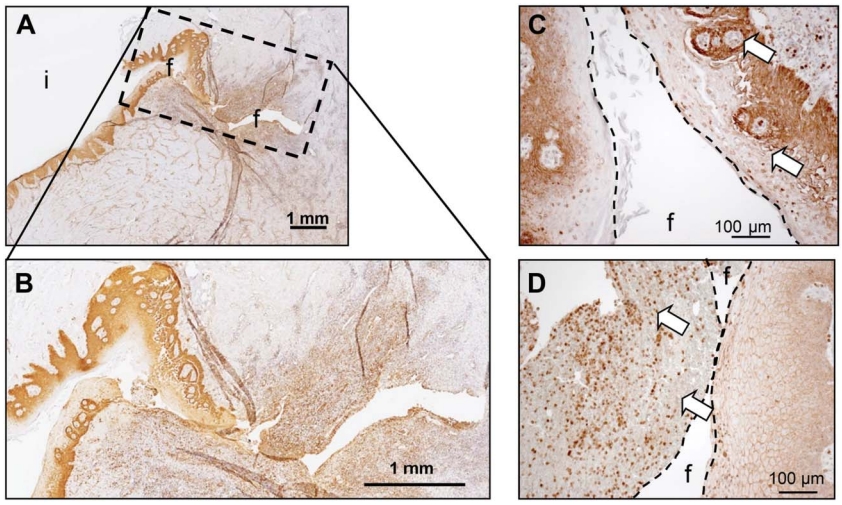

FIGURE 1. MMP-9 expression in intestinal mucosa of patients with perianal fistulae. Surgically resected colonic tissue specimens were immunohistochemically stained for MMP-9 (brown staining). (A and B) MMP-9 alongside fistula tract (merged ×5 magnification). MMP-9 staining (C) in epithelial cells of deformed crypts (arrows) and (D) in inflammatory infiltrates adjacent to the fistula tract (arrows). Images representative of all investigated samples (n = 5). Scales as indicated. Dotted line, fistula tract; f, fistula lumen; i, intestinal lumen.

TABLE 3. Difference in Serum Biomarkers in Patients with Penetrating (Montreal B3) CD and HC

		HC			CD B3 Patients			
Enzyme Involved	Neopeptide	N	Mean ± SD (ng/mL)	Lower and Upper 95% CI of Mean	N	Mean ± SD (ng/mL)	Lower and Upper 95% CI of Mean	*P*, B3 Versus HC
MMP-9	C3M	10	12.27 ± 2.11	10.75–13.78	22	23.29 ± 12.50	17.74–28.83	0.0005
MMP-9	BGM	10	19.67 ± 6.71	14.87–24.57	22	29.41 ± 24.06	18.74–40.08	ns
MMP-2/9	C6M	10	17.67 ± 6.27	13.18–22.16	20	27.75 ± 24.30	16.37–39.12	ns
MMP-2/9	LAM	10	24.25 ± 32.84	0.758–47.74	20	9.02 ± 5.66	6.37–11.67	ns
MMP-2/9/13	C1M	10	43.72 ± 16.13	32.19–55.26	20	91.4 ± 105.3	42.1–140.7	ns

Statistical analysis was performed using unpaired *t* test with Welch's correction. Twenty of 22 serum samples from the B3 group were tested for C6M, LAM, and C1M because of limited serum sample volume.
ns, not significant.

addition, although the difference in serum levels of BGM, biglycan fragment generated by MMP-9, between CD B3 patients and HC failed to reach statistical significance, we observed a good correlation between serum levels of C3M and BGM ($r^2 = 0.8038$, $P < 0.0001$) in CD B3 patients (data not shown).

We next focused on C3M peptide and compared its serum levels in patients with nonstricturing and nonpenetrating CD (B1 group), stricturing CD (B2 group), and perianal fistula CD (B3p group) with levels in serum from HC. None of the other CD patient groups showed a significant difference in the mean value of C3M serum levels when compared with HC as shown in Figure 2 and Table 4. Interestingly, the mean value of serum levels of C3M was not increased in the CD B3p patients compared with levels observed in HC. Although CD B3p patients have perianal fistulae, they have less severe disease compared with B3 patients who have abdominal fistulae with abscesses, indicating that C3M could also be a biomarker of penetrating CD severity. The mean value of C3M levels in CD B3 patients was statistically different when compared with B1 ($P = 0.0056$), B2 ($P = 0.0003$), and B3p CD ($P = 0.0004$) subgroups, indicating that increased C3M serum levels are potential biomarkers of penetrating CD.

CALY-001 Monoclonal Antibody is a Potent and Selective Inhibitor of Human and Mouse MMP-9

MMP-9-specific fully human monoclonal antibodies were generated by phage display technology using recombinant human MMP-9 proteins. Single-chain variable fragments (scFv) were selected by in vitro screening for target binding and inhibition of substrate proteolysis. After reformatting clones of interest to human IgG4, candidates were tested for potency, efficacy, species specificity, and selectivity versus other MMP family members. The selection process yielded CALY-001, which inhibits human and mouse MMP-9-mediated cleavage of the physiologically relevant substrate gelatin (partially denatured collagen) with similar potency and efficacy: $IC_{50} = 0.97 \pm 0.16$ nM for recombinant human MMP-9 and $IC_{50} = 1.27 \pm 0.2$ nM for recombinant mouse MMP-9, with 100% efficacy. CALY-001 exhibits binding to activated MMP-9, with $K_D = 12$ nM, but not to pro-MMP-9, with $K_D > 15$ μM (data not shown). CALY-001 showed greater than 100-fold selectivity for human MMP-9 versus 8 other tested MMP family members including MMP-2, which is highly homologous to MMP-9 (Fig. 3A). Cell-free enzymatic assays using either recombinant pro-MMP-9 or APMA-activated MMP-9

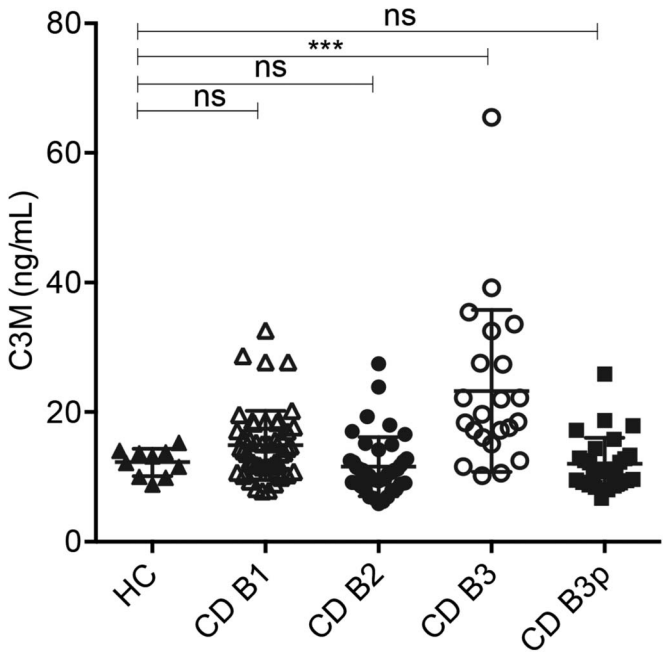

FIGURE 2. Serum levels of neopeptide C3M in subsets of patients with CD and HC. Nonstricturing and nonpenetrating CD (B1; open triangle; n = 50), stricturing CD (B2; closed circle; n = 41), penetrating CD (B3; open circle; n = 22), CD with perianal fistula (B3p; closed square; n = 29), and HC (closed triangle; n = 10). Statistical analysis was performed using one-way analysis of variance with Dunnett's multiple comparison posttest to reveal any significant difference between the groups. ns, not significant.

TABLE 4. C3M Serum Levels in Patients with Montreal class B1, B2, and B3 CD and HC

Groups of Subjects	N	C3M Mean ± SD (ng/mL)	C3M Lower & Upper 95% CI of Mean	C3M *P* CD Patients Versus HC
CD B1	50	14.87 ± 5.36	13.35–16.40	ns
CD B2	41	11.60 ± 4.53	10.17–13.03	ns
CD B3	22	23.29 ± 12.50	17.74–28.83	0.0005
CD B3p	29	12.02 ± 4.01	10.50–13.55	ns
HC	10	12.27 ± 2.11	10.75–13.78	

Statistical analysis was performed using one-way analysis of variance with Dunnett's Multiple Comparison Posttest.
ns, not significant.

revealed that CALY-001 is a pure inhibitor of enzymatic activity behaving as noncompetitive inhibitor, as the IC_{50} values generated against the enzyme activity on a peptide substrate were not substantially affected by substrate concentrations ranging from 1 to 7.5 μM (data not shown). CALY-001 inhibition of natural forms of MMP-9 was evaluated using MMP-9 monomers, dimers, and NGAL/MMP-9 complexes purified from human neutrophils. As shown in Figure 3B, CALY-001 efficiently inhibited cleavage of DQ-gelatin by MMP-9 monomers with an IC_{50} = 1.37 nM, MMP-9 dimers with an IC_{50} = 0.45 nM, and NGAL/MMP-9 with an IC_{50} = 1.77 nM.

CALY-001 Anti-MMP-9 Antibody Decreases Intestinal Fibrosis in a Mouse Model

Effect of MMP-9 inhibition was assessed in the heterotopic transplant mouse model of intestinal fibrosis by starting treatment with anti-MMP-9 antibodies CALY-001 or AB-0046-h4 5 days after transplantation. In this study, we have used AB-0046-h4 as a comparator. Body weight remained unchanged in animals treated with anti-MMP-9 antibody, CALY-001, or AB-0046-h4, and in animals treated with isotype control (data not shown). Grafts were explanted 14 days after transplantation, and collagen production and deposition were analyzed on Sirius Red staining under transmission light and under polarizing light in 2 independent experiments, and compared with freshly isolated intestinal resections. Results of experiment 1 are shown in Figure 4. Freshly isolated intestinal resections were characterized by an open lumen and distinctive epithelial crypts (Fig. 4A, B). In the isotype control–treated group, at day 14 after transplantation, the lumen of intestinal grafts was fully obstructed by granular tissue and fibrotic material (Fig. 4D, E). In the anti-MMP-9 antibody-treated groups, the lumen of the intestinal grafts was only partially obstructed, and some crypt structures were still present. Freshly isolated intestinal samples showed a thin collagen layer adjacent to the submucosa (Fig. 4B, C). The collagen layer was much thicker in grafts harvested from the isotype control–treated group: a massive accumulation of collagen was observed, spreading from the submucosa to the occluded lumen (Fig. 4E, F). In contrast, in grafts harvested from anti-MMP-9 antibody-treated mice, the collagen layer was only slightly thicker than that observed in freshly isolated intestinal samples (Fig. 4H, I, L, M). Freshly isolated intestinal samples showed long-chained collagen (red stain) bordering the submucosa (Fig. 4C). In grafts from isotype control–treated mice, increased short-chain collagen (green stain) was observed in the submucosa and in the luminal occlusion as a sign of an ongoing fibrotic process (Fig. 4F). In contrast, long-chain collagen (red stain) was associated with a thinner collagen layer in grafts from mice treated with anti-MMP-9 antibody CALY-001 and AB-0046-h4 as a sign of lower accumulation of newly

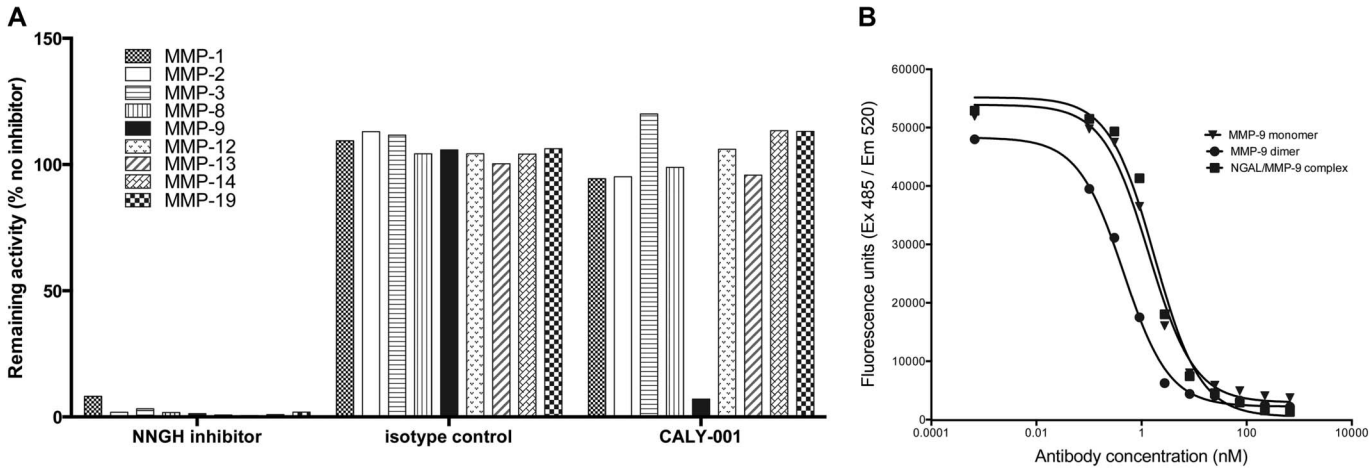

FIGURE 3. Characterization of MMP selectivity of CALY-001. A, Neutralization of catalytic domain of various human MMPs by MMPs broad inhibitor (NNGH), by isotype control antibody, or by CALY-001 anti-MMP-9 antibody. Remaining activities were normalized to conditions where no inhibition was applied. B, Neutralization of natural forms of MMP-9 by CALY-001. CALY-001-mediated inhibition of DQ-gelatin degradation by MMP-3-activated human monomeric MMP-9 (triangles), dimeric MMP-9 (circles), and NGAL-MMP-9 complex (squares) derived from human neutrophils was evaluated over a dilution series of antibody stock solution. Curves shown are representative of 3 independent experiments.

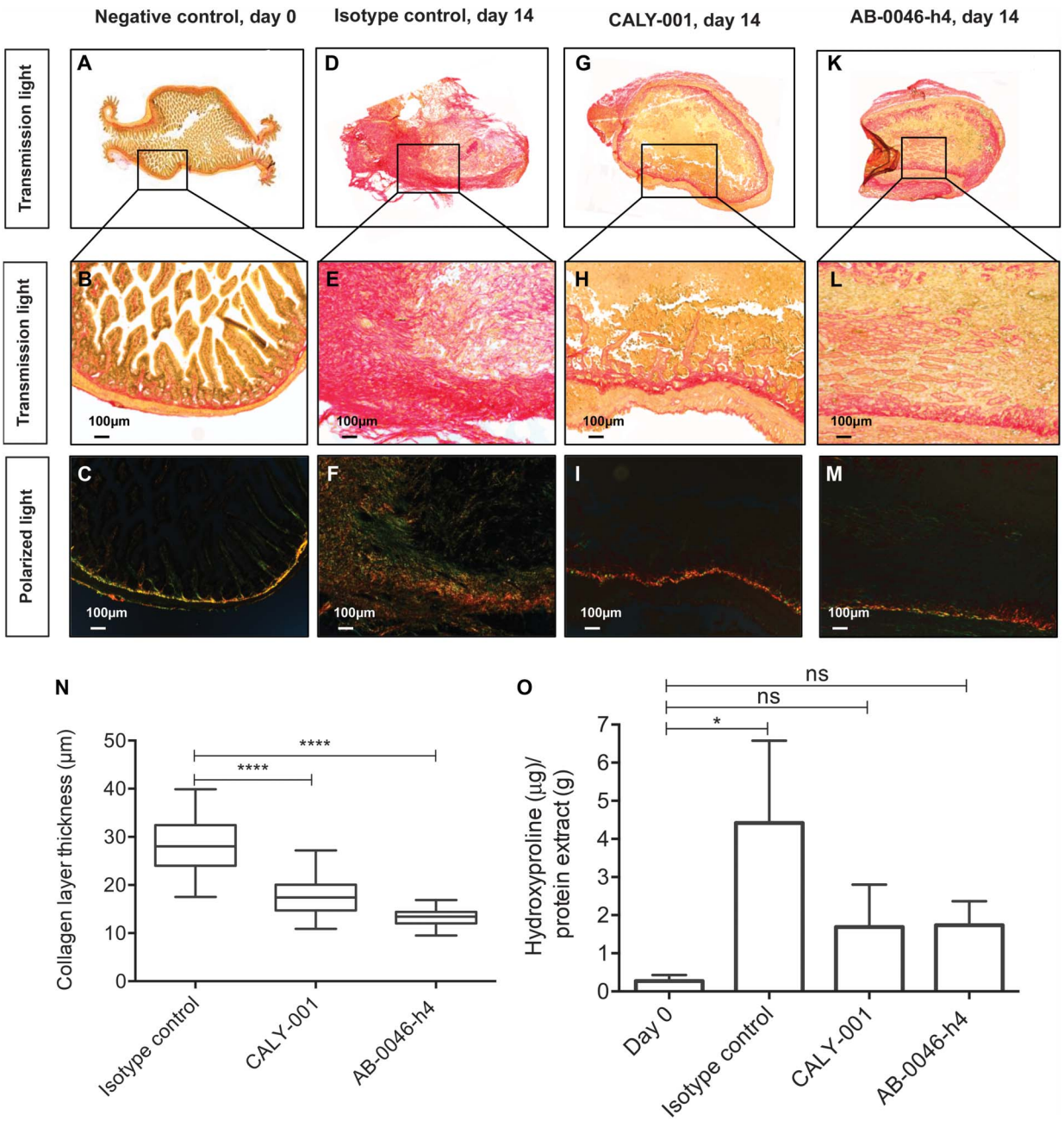

FIGURE 4. Anti-MMP-9 antibody treatment reduces collagen deposition in intestinal grafts. Representative images of cross-sections of freshly isolated small intestine (A–C) and of grafts explanted at day 14 after transplantation from mice treated with isotype control (D–F), with CALY-001 anti-MMP-9 antibody (G–I), or with AB-0046-h4 anti-MMP-9 antibody (K–M). Cross-sections were stained with Sirius red and observed under transmitted light microscopy (A, B, D, E, G, H, K, L) and polarized light (C, F, I, M). Pictures B, C, E, F, H, I, L and M are ×10 magnifications of sections A, D, G and K (merged ×5 magnification). (N) Collagen layer thickness was determined using Sirius red stained sections from freshly isolated small bowel at day 0 and from grafts isolated 14 days after transplantation. Median, maximum, and minimum values are shown. One hundred ninety-four measures were performed using 13 grafts for the day 0 group. At day 14 after transplantation, 157 measures were performed using 10 grafts for the CALY-001-treated group, 159 using 12 grafts for the isotype control–treated group, and 213 using 15 grafts for the AB-0046-h4–treated group. Statistical comparisons of anti-MMP-9-treated groups versus the isotype control–treated group were performed using the one-way ANOVA with Dunnett's multiple comparison posttest. O, Hydroxyproline was determined using protein extracts of sections from freshly isolated small bowel resections (day 0, white bar) and from grafts isolated 14 days after transplantation (black bars) from experiment 2. Hydroxyproline was quantified in 7 freshly isolated small bowel resections (day 0 group). At day 14 after transplantation, measures were performed using 6 grafts from the isotype control group and CALY-001- or AB-0046-h4–treated group. Plots show group mean ± SEM. Statistical comparison of groups was performed using one-way ANOVA with Dunn's method. *P* value designations are as follows: *< 0.05, **< 0.01, ***<0.001, ****< 0.0001, ns for nonspecific. ANOVA, analysis of variance.

synthesized collagen (Fig. 4I, M). Quantitative analysis confirmed a significantly thinner collagen layer in grafts from mice treated with anti-MMP-9 antibodies compared with those treated with isotype control (Fig. 4N). Quantification of collagen-specific amino acid hydroxyproline confirmed lower collagen amounts in grafts from mice treated with anti-MMP-9 antibodies compared with those treated with isotype control (Fig. 4O). Collectively, these results provide evidence that anti-MMP-9 antibodies can control active intestinal fibrotic process.

Expression of MMP-9 and TIMP-1 in Intestinal Grafts is Not Affected by Anti-MMP-9 Antibody Treatment

Analysis of the mRNA expression of *Mmp9* and its natural inhibitor *Timp1* was performed in grafts isolated 14 days after transplantation. Transplants isolated from isotype control–treated mice showed a significant increase in *Mmp9* and *Timp1* mRNA experssion levels related to *Gapdh* when compared with freshly isolated small bowel resections (Fig. 5A, B). Interestingly, *Mmp9* and *Timp1* mRNA expression levels were similar in grafts from isotype control- or from anti-MMP-9-treated groups (Fig. 5A, B).

MMP-9 protein expression was analyzed by IHC conducted on serial sections of freshly isolated small bowel resections or graft explanted at day 14 after transplantation using anti-mouse MMP-9 antibody (Fig. 6A). Increased MMP-9 staining was detected in 14-day grafts (Fig. 6A, panels c–h) when compared with freshly isolated small bowel (Fig. 6A, panels a, b), whereas treatment with anti-MMP-9 antibodies had no effect on MMP-9 protein expression levels (Fig. 6A, panels e–h) when compared with isotype control–treated group (Fig. 6A, panels c, d). Quantification of MMP-9 positive cells showed that their number was increased at day-14 after transplantation, as compared with freshly isolated bowel resection (day 0) and remained unchanged regardless of the antibody treatment (Fig. 6B).

MMP-9 Activity is Increased in Intestinal Grafts and Modulated by Anti-MMP-9 Antibody Treatment

Gelatinase activity present in homogenates from freshly isolated small bowel resections and from day-14 grafts explanted from mice treated with either isotype control or anti-MMP-9 antibodies was assessed by zymography (Fig. 6C) and by ELISA (Fig. 6D). It is worth noting that gelatin-based zymography uses a polyacrylamide gel-based electrophoretic approach that dissociates the complex made between antibody and antigen; thus, antibody-mediated inhibition cannot be revealed by this method. In contrast, the ELISA method preserves the immune complex and enables the detection of antibody-mediated inhibition. Moreover, zymography provides semiquantitative information on total MMP-9 amounts, with both pro-MMP9 and MMP-9 species being revealed, whereas ELISA enables the quantification of active MMP-9. Very low MMP-9 amounts were found by zymography in homogenates from all freshly isolated small bowel resections (day 0), whereas all day-14 explants exhibited increased total MMP-9 (Fig. 6C), which were mainly pro-MMP-9 species (data not shown). Endowed with higher sensitivity (1 pg/mL), the MMP-9 activity ELISA assay revealed that mature MMP-9 was 5.3-fold increased in grafts isolated from the isotype control group compared with levels measured in freshly isolated small bowel resections (Fig. 6D). Although not statistically significant because of the small sample number and the heterogeneity of data obtained from the isotype control–treated group, the mean value of mature MMP-9 was reduced by 2-fold in grafts from CALY-001-treated

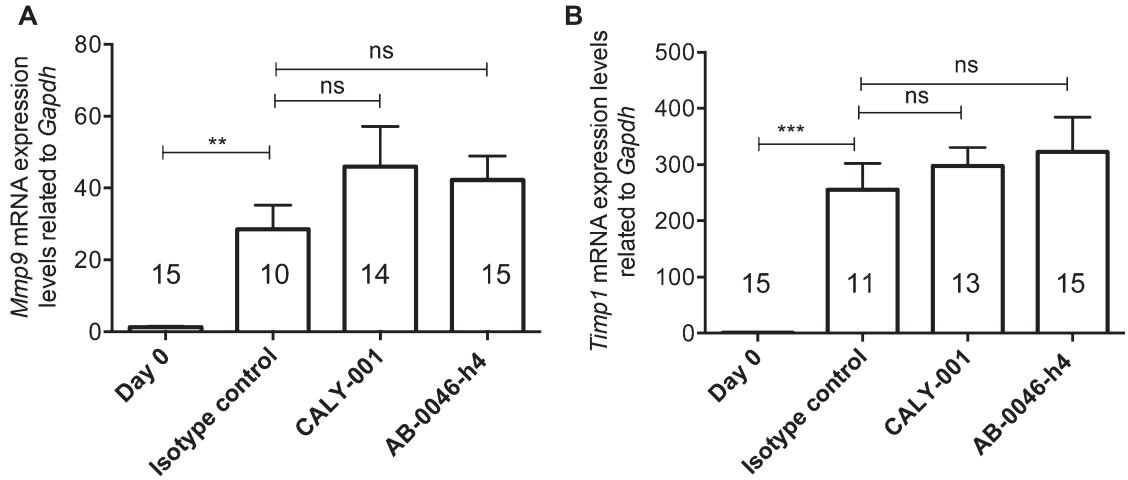

FIGURE 5. *Mmp9* and *Timp1* mRNA expression in intestinal grafts. mRNA expression levels of *Mmp9* (A) and of *Timp1* (B) in freshly isolated bowel resections (day 0) or in grafts isolated 14 days post implantation from mice treated either with isotype control or with anti-MMP-9 antibody (CALY-001 or AB-0046-h4). Results are reported as mean expression levels related to GAPDH ± SEM. Number of grafts analyzed per group are indicated. Statistical comparisons of means between each group and the isotype control–treated group were assessed by Kruskal–Wallis analysis. ns for not significant. *P* value designations are as follows: *< 0.05, **< 0.01, ***< 0.001, ****< 0.0001.

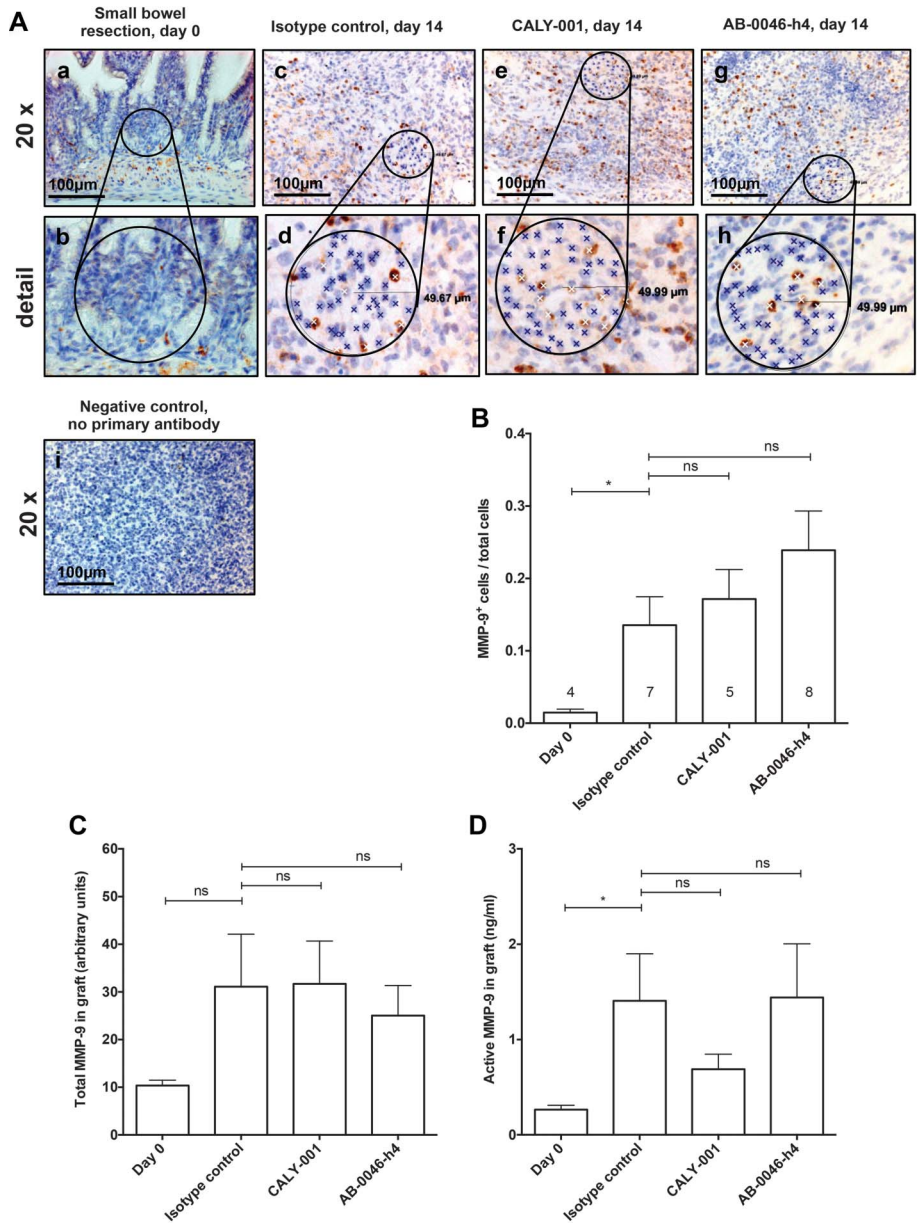

FIGURE 6. MMP-9 expression in intestinal grafts. A, IHC was conducted on serial sections of freshly isolated graft or graft explanted at day 14 after transplantation using anti-mouse MMP-9 antibody (brown) and hematoxylin (blue), as counter staining. Staining was conducted on sections of freshly isolated bowel resections (a, b) and of grafts isolated from mice treated with isotype control (c, d) or with anti-MMP-9 antibody (CALY-001 in e, f or AB-0046-h4 in g, h). IHC of a section from a non-treated animal (i) was the negative control. Negative control staining was performed on section of graft explanted at day 14 after transplantation in absence of primary antibody. MMP-9 positive (MMP-9$^+$) cells (yellow crosses in c–h) were counted in areas of 50 µm in freshly isolated small bowel resections and in day 14 grafts. The ratios between the number of MMP-9$^+$ cells and the number of total cells (nuclei labelled with blue and yellow crosses) were reported in panel B. Numbers of areas analyzed are indicated in graph columns. MMP-9 activity in intestinal grafts. Equal amounts of total protein extracted from homogenates of freshly isolated small bowel resections (day 0) or of grafts isolated 14 days post implantation from mice treated either with isotype control or with anti-MMP-9 antibody (CALY-001 or AB-0046-h4) were analyzed by zymography for total MMP-9 (C) and by ELISA for mature MMP-9 (D). Results are reported as mean MMP-9 activities ± SEM. An n of 5 grafts per group were analyzed. Statistical comparisons between each group and the isotype control–treated group were assessed using Mann–Whitney test. ns for not significant, *for $P < 0.05$.

mice when compared with grafts from the isotype control group. In contrast, treatment by AB-0046-h4 failed to reduce active MMP-9 (the mean value ± SEM = 1.44 ± 0.56 ng/mL; Fig. 6D). It is worth noting that, unlike the CALY-001-treated group, the AB-0046-h4–treated group exhibited high heterogeneity in MMP-9 activity levels.

Anti-MMP-9 Antibodies Co-localize with Basement Membranes in Intestinal Grafts

The distribution of the injected antibodies after heterotopic transplantation was investigated in histological cross-sections of grafts. IHC with polyclonal rabbit anti-human IgG antibody revealed intense staining in harvested grafts from mice treated with CALY-001, AB-0046-h4, or isotype control (see Supplemental Fig., panels A–I, Supplemental Digital Content, http://links.lww.com/IBD/B293) as compared with the negative control (see Supplemental Fig., panel K, Supplemental Digital Content, http://links.lww.com/IBD/B293). Although epithelial structure was lost in heterotopic intestinal grafts, both CALY-001 and AB-0046-h4 were also localized at sites where the epithelial basement membrane of the former crypt area was expected (see Supplemental Fig., panels E and H, Supplemental Digital Content, http://links.lww.com/IBD/B293). Both anti-MMP-9 antibodies, CALY-001 and AB-0046-h4, co-localized with the vascular basement membrane (see Supplemental Fig., panels F and I, Supplemental Digital Content, http://links.lww.com/IBD/B293). Less human IgG staining co-localized with basement membranes on treatment with isotype control (see Supplemental Fig., panels B and C, Supplemental Digital Content, http://links.lww.com/IBD/B293). These results demonstrate an accumulation of anti-MMP-9 antibodies in both epithelial and vascular basement membranes, probably resulting from the expression of MMP-9 at these locations.

Expression of TGF-β mRNA and TGF-β Protein is Increased in Intestinal Grafts and Not Altered by Anti-MMP-9 Antibody Treatment

Next we analyzed TGF-β mRNA and TGF-β protein expression in intestinal transplants by real-time PCR and ELISA. *Tgfb1* mRNA expression was increased in day-14 grafts compared with freshly isolated small bowel resections. However, it was equivalent in day-14 grafts from anti-MMP-9–treated groups compared with isotype control–treated animals (Fig. 7A). Similarly, TGF-β protein expression was increased in day-14 grafts compared with freshly isolated small bowel resections, but not modulated by anti-MMP-9 antibody treatment (Fig. 7B). Modulations of the active fraction of TGF-β exhibited the same pattern (data not shown). Together, these data suggesting that the antifibrotic effect observed in this model are not mediated by control of TGF-β.

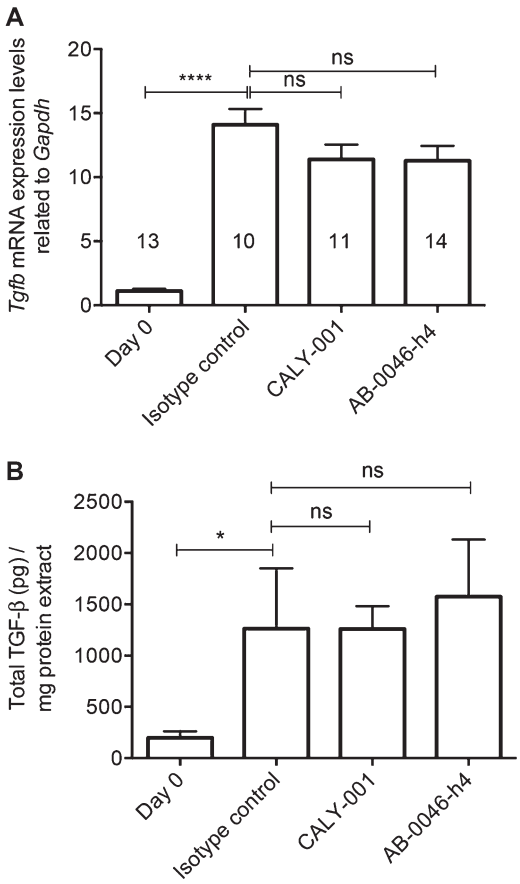

FIGURE 7. TGF-β mRNA and protein expression in intestinal grafts. mRNA and protein expression levels of TGF-β were quantified in freshly isolated bowel resections (day 0) and in grafts isolated 14 days post implantation from mice treated either with isotype control or with anti-MMP-9 antibody (CALY-001 or AB-0046-h4). A, mRNA expression levels are reported as mean expression levels related to *Gapdh* ± SEM. Numbers of grafts analyzed per group are indicated within column of the graph. B, Total TGF-β levels are reported as mean MMP-9 activities ± SEM. An n of 5 grafts per group were analyzed. Statistical comparisons of means between each group and the isotype control–treated group were assessed by Kruskal–Wallis analysis. ns for not significant, *for $P < 0.05$.

E-cadherin and α-SMA Expressions are Modulated by Graft Transplantation, but Not Affected by Anti-MMP-9 Treatment

We investigated the influence of anti-MMP-9 treatment on E-cadherin and α-SMA expressions, both being hallmarks of EMT, which play an important role in organ fibrosis. IF with anti-mouse E-cadherin antibody revealed intense staining in intestinal epithelial cells of freshly isolated small intestinal resection (Fig. 8A). In the isotype control–treated group, at day 14 after transplantation, the loss of crypt structures and luminal occlusion was complete and E-cadherin staining was lost (Fig. 8B). As expected, labeling of freshly isolated small intestinal resection with anti-mouse α-SMA antibody showed minor staining, limited to subepithelial myofibroblasts in the crypts (Fig. 8E). α-SMA is a marker gained in myofibroblasts during intestinal fibrosis. Expression of α-SMA in grafts at day 14 after transplantation was increased and rather patchy (Fig. 8F). These 2 findings are in agreement with the expected results on the induction of fibrosis, i.e., decreased E-cadherin and increased α-SMA expressions. However, treatment with either anti-MMP-9 antibody did not trigger any significant change in expression of E-cadherin (Fig. 8C and D) or in α-SMA (Fig. 8B, panel g and h). These results suggest that the antifibrotic effect observed is not mediated by control of EMT.

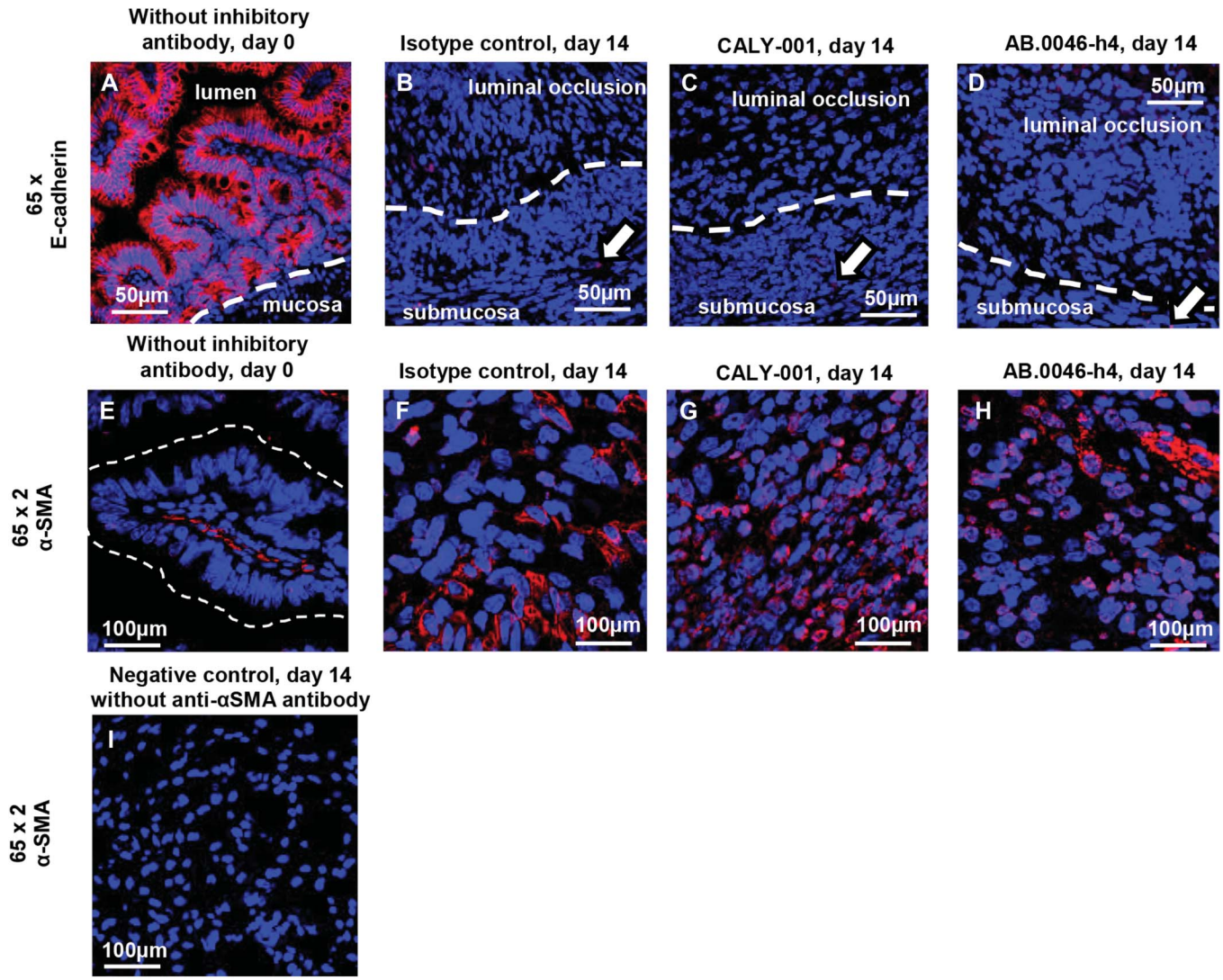

FIGURE 8. Representative images of cross-sections of freshly isolated small intestine and of grafts explanted at day 14 after transplantation from mice treated with isotype control (B and F), with anti-MMP-9 antibody CALY-001 (C and G), or AB-0046-h4 (D and H). IF staining of E-cadherin (red) and of DAPI (blue) are shown in pictures A–D. IF staining of α-SMA (red) and of DAPI (blue) are shown in pictures E–H. (I) Negative control, graft explanted at day 14 after transplantation stained in absence of primary antibody. The original ×65 magnification was 2-fold enlarged with the LAS AF software. Each image is representative for 5 samples investigated. Dashed line, crypt cut along the long axis. Arrow, erythrocytes.

DISCUSSION

Based on the observed dysregulation of MMP-9 expression and activity in the gut of active CD and UC, MMP-9 is considered as a critical component of intestinal inflammation in IBD, but less is known concerning the role of MMP-9 in penetrating or stricturing CD. In this report, we describe a serological biomarker of MMP-9 enzymatic activity, the C3M neopeptide generated by MMP-9-mediated proteolytic cleavage of collagen III, whose levels are significantly elevated in penetrating CD when compared with other CD patient subgroups. We propose that this new biomarker could be used to identify patients who are more susceptible to developing complex fistulae and who could more likely respond to anti-MMP-9 treatment. In a parallel approach, we have generated an anti-MMP-9 antibody, CALY-001, and have evaluated its efficacy in a recently developed mouse model of intestinal fibrosis head to head with AB-0046-h4 used as a comparator. We show that inhibiting MMP-9 significantly reduces collagen deposition and intestinal tissue remodeling. This anti-fibrotic effect, associated with the anti-inflammatory effect of MMP-9 inhibitor described in the DSS-colitis model by Marshall and colleagues using AB-0046,[32] supports the development of an anti-MMP-9 antibody in patients with penetrating CD.

Patients with penetrating CD represent an unmet clinical need, since none of the current therapies results in widespread remission or in fistulae closure. TNF antagonists are the most effective drugs for penetrating CD, yet only one-third of the

patients will respond to anti-TNF antibody treatments and another third will lose response during the first year of treatment because of intolerance or appearance of antidrug antibodies.[37,38] This results in a cumulative risk of intestinal resection of 70% during the first 15 years after diagnosis. We suggest that an anti-MMP-9 antibody has advantages over current treatment options for penetrating CD because simultaneously targeting inflammation, tissue destruction, and fibrosis that drive fistula formation may lead to superior efficacy than that achieved with classical immunosuppressive agents. The implication of MMP-9 as a primary disease driver in IBD is unequivocal. Several reports describe upregulation of MMP-9 expression and activity in inflamed mucosa or serum of patients with IBD[39,40] and recent safety and efficacy data of Gilead Sciences's anti-MMP-9 antibody, GS-5745, in a multicenter, double-blind, phase Ib study in patients with moderate to severe UC support the therapeutic promise of an anti-MMP-9 antibody.[40a]

Enhanced MMP-9 transcripts and protein levels were described in lamina propria mononuclear cells, granulocytes, and giant cells in CD fistula specimens with acute inflammation and granulation tissue. Fistulae were also shown to express active MMP-9,[13,41,42] indicating that MMP-9 may contribute to fistula formation. Our IHC analysis of fistula specimens shows that MMP-9 expression was closely associated with epithelial and inflammatory cells adjacent to the fistula tracks, which is in agreement with our previous finding where we could show increased MMP-9 protein expression in colonic lamina propria fibroblasts from fistula patients compared with control fibroblasts.[43] These observations indicate the presence of substantial amounts of MMP-9 associated with fistulae that trigger excessive production and release of tissue-specific protein fragments, locally as well as in the circulation. Proteolytic degradation fragments measured in serum have received increased attention because of their diagnostic and prognostic potential in diseases. For example, in the phase III LITHE biomarker study in rheumatoid arthritis, it was possible, using the C2M and C3M biomarkers of joint tissue remodeling, to identify the profiles of responders and nonresponders to the anti-IL-6R antibody tocilizumab.[44] Recently, Mortensen and colleagues reported that the biomarkers VICM (degradation fragment of citrullinated protein vimentin), C3M, C1M, and C4M are potential biomarkers that differentiate IBD from non-IBD patients, whereas both VICM and C3M may also be biomarkers that differentiate patients with CD from patients with UC.[45] Mortensen and colleagues also found that BGM is highly elevated in UC compared with CD. In this study, we investigated the profile of specific MMP-9-generated protein products in serum from CD patients with inflammatory, fibrostenotic or penetrating phenotype to assess whether serum levels of specific MMP-9 degradation products reflect these different pathogenic features of CD. Among the 5 peptides quantified, C1M, C3M, C6M, LAM, and BGM, only C3M, which results from MMP-9-specific degradation of type III collagen, was significantly elevated in patients with penetrating CD when compared with HC and with other CD subgroups, indicating that C3M has the potential to be a biomarker of MMP-9 activity associated with complex fistulae. In our study, mean value of C3M serum levels in CD B3 patients and HC were lower than values reported by Mortensen and colleagues in patients with CD and UC and in HC. It is worth noting that their data were obtained from 2 independent cohorts of patients with CD, in which only 7% and 10% of patients had penetrating disease. The heterogeneity within the patient cohorts may account for the difference observed since C3M levels were assessed using identical ELISA technology in both studies. It also worth mentioning that Mortensen and colleagues reported the highest levels of C3M in patients with UC, suggesting that similar MMP-9-mediated ECM remodeling processes take place in UC and in the CD B3 group.

In contrast, serum levels of another MMP-9-specific neoepitope, BGM, were similar in patients with penetrating CD when compared with other CD patient groups. BGM peptide is derived from biglycan (BGN), which is a secreted proteoglycan belonging to the family of small leucine-rich proteoglycans present in sites affected by fibrosis and which controls lateral assembly of collagen fibers.[46,47] The fact that circulating levels of C3M, but not of BGM, were found associated with penetrating CD indicates that MMP-9 activity and the presence of collagen type III provide a unique combination relevant for the CD B3 patient group. Indeed, quantification of circulating C3M levels seems to be a powerful indicator of fistulae since past attempts to reveal a relationship of MMP-9 activity in inflamed CD tissue with the co-presence of fibrosis or fistula by gelatin zymography failed.[41] Similarly, collagen contents in resected strictured intestine of patients with CD were found similar, regardless of the presence of fistula.[48] A systemic C3M biomarker has the potential to serve as marker for the development of fistula that cannot be easily identified clinically. These findings warrant further studies aiming at exploring the potential use of C3M to assess severity of penetrating CD and efficacy of MMP-9 inhibitor.

The anti-fibrotic effect of anti-MMP-9 antibodies was successfully characterized in our model of intestinal fibrosis. A model recapitulating the pathogenesis of intestinal fistula does not exist. Rat models in which fistula are surgically created have been used to assess repair agents such as chitosan hydrogel,[49] stable gastric pentadecapeptide BPC 157[50] or stem cell therapy.[51] Unfortunately, these models are not suitable for testing agents having the potential to control cellular and molecular processes leading to fistula development as those are bypassed in the surgical models. The association of aberrant chronic inflammation and repair processes resulting in collagenous tissue has been linked with fistula development. Therefore, studies using pharmacological agents in intestinal inflammatory models and in intestinal fibrosis models would suggest that they could show amelioration or prevention of fistula development. Since both anti-MMP-9 antibodies, AB-0046-h4[32] and CALY-001 (data not shown) were shown to reduce disease severity in a DSS-induced mouse model of intestinal inflammation, it was logical to assess the antifibrotic activity of our anti-MMP-9 antibody in a model of intestinal fibrosis, using AB-0046-h4 as a reference compound. Heterotopic transplantation of small bowel resections in mice was followed by fibrosis of the intestinal wall. Sirius Red staining confirmed

a significant increase of collagen layer thickness in day-14 transplants and revealed a diffused network of fibrils in the obliterated lumen. Reverse transcription polymerase chain reaction, IHC, and zymography experiments showed that MMP-9 gene and protein expression as well as MMP-9 activity were significantly increased in day-14 transplants compared with freshly isolated small bowel resections. Therapeutic dosing of 2 nonrelated anti-MMP-9 antibodies in this model showed that inhibiting MMP-9 significantly restrains fibrogenesis, as revealed by a significant decrease of the thickness of the collagen layer and hydroxyproline levels in day-14 grafts compared with grafts isolated from isotype control–treated mice. The fact that both antibodies used in this study inhibit MMP-9 with a different mechanism of action strengthens these results. CALY-001 is an inhibitor of MMP-9 enzymatic activity, whereas AB-0046-h4 is an inhibitor of pro-MMP-9 activation leading to decreased MMP-9 activity. Moreover, we observed that anti-MMP-9 antibodies co-localized with epithelial and vascular basement membranes in day-14 grafts, proving that both blocking antibodies have reached the site where their target exerts its enzymatic activity. Using an ELISA assay, we observed a trend of anti-MMP-9 antibody–mediated inhibition of MMP-9 activity in grafts of mice treated with CALY-001. However, we could not obtain statistical significant differences in activity means between CALY-001 and isotype control–treated mice, probably due to the small number of mice tested and to the heterogeneity in data obtained in the isotype control group. Serum levels of C3M were very low in all groups of mice, certainly because fibrosis is limited to the intestinal grafts in this model and C3M locally produced is diluted in the blood.

Studies using either *Mmp9*-deficient mice in a model of obstructive nephropathy[52] or MMP-9 neutralizing antibody in murine unilateral ureteral obstruction model have shown a reduction of kidney fibrosis[53] mediated by (1) inhibition of tubular cell EMT, an major source of myofibroblast in kidney fibrosis; (2) infiltration of interstitial macrophage, a major source of MMPs and profibrotic cytokines. In addition, MMP-9 itself has been shown to induce the entire course of renal tubular cell EMT through cleavage of collagen and laminin and disruption of E-cadherin/β-catenin–mediated cell-to-cell adhesion complex,[11,54] leading to loss of tubular basement membrane integrity. EMT is characterized by loss of epithelial markers such as E-cadherin and cytokeratin, and by nuclear translocation of β-catenin accompanied by de novo expression of mesenchymal markers typically α-SMA. A number of EMT characteristic events were documented in and around fistula tracts supporting a role for EMT in the pathogenesis of CD-associated fistulae.[55] It was logical to speculate that similar mechanisms may account for the intestinal fibrosis observed in the heterotopic intestinal transplant model. Our results showed that collagen deposition in the day-14 grafts was correlated with loss of E-cadherin and induction of α-SMA expression. However, the therapeutic effect observed with anti-MMP-9 antibodies was not correlated neither with restored E-cadherin nor decreased α-SMA expression in intestinal grafts indicating that fibrosis in these grafts was controlled by another mechanism. TGF-β is known to play a crucial role in tissue remodeling and inflammation in the gut. TGF-β promotes collagen production by smooth muscle cells isolated from CD tissue[56] and inhibits intestinal epithelial cell proliferation, a process that may inhibit re-epithelialization after surface injury.[57] In addition, TGF-β is activated by MMP-9-mediated proteolytic cleavage of latent TGF-β.[58] We therefore explored whether the antifibrotic activity of the anti-MMP-9 antibody treatment was associated with a decreased TGF-β production or activity. We observed that total and active TGF-β levels were increased in day-14 grafts, but these levels were not altered by anti-MMP-9 antibody treatments. Using the same mouse model of intestinal fibrosis, we found that treatment with pirfenidone led to the decrease of collagen deposition in grafts which correlated with a significantly reduction of TGF-β expression.[25] Grafts from mice treated with pirfenidone showed a significant decrease in *Acta2* (α-SMA) and *Mmp9* mRNA expression compared with vehicle, suggesting that the antifibrotic effect of pirfenidone observed in this model was mediated by altered MMP-9 expression. The fact that, in this study, we could not correlate the reduction in collagen deposition in day-14 grafts mediated by 2 independent anti-MMP-9 antibodies with a local molecular process suggests that graft-associated fibrosis might have been controlled by a systemic response. Although we could not reveal the mechanism by which anti-MMP-9 antibodies have controlled the collagen deposition in day-14 intestinal grafts, our results warrant further studies in other models of intestinal fibrosis.

In this report, we demonstrate the association between an MMP-9 degraded type III collagen fragment C3M and penetrating CD indicating that C3M has the potential to be a marker of the development of fistulae. In addition, we demonstrated that antibody-mediated inhibition of MMP-9 reduced collagen deposition in grafts from a heterotopic intestinal transplant model, suggesting that inhibition of MMP-9-mediated proteolysis could be an effective means of dampening fibrosis that contributes to fistula development.

ACKNOWLEDGMENTS

The authors thank André Fitsche (Institute of Surgical Pathology, University Hospital Zurich, Zurich, Switzerland) for his support with IHC.

REFERENCES

1. Cosnes J, Cattan S, Blain A, et al. Long-term evolution of disease behavior of Crohn's disease. *Inflamm Bowel Dis.* 2002;8:244–250.
2. Silverberg MS, Satsangi J, Ahmad T, et al. Toward an integrated clinical, molecular and serological classification of inflammatory bowel disease: report of a Working Party of the 2005 Montreal World Congress of Gastroenterology. *Can J Gastroenterol.* 2005;19(suppl A):5A–36A.
3. Schwartz DA, Loftus EV Jr, Tremaine WJ, et al. The natural history of fistulizing Crohn's disease in Olmsted County, Minnesota. *Gastroenterology*. 2002;122:875–880.
4. Loftus EV, Schoenfeld P, Sandborn WJ. The epidemiology and natural history of Crohn's disease in population-based patient cohorts from North America: a systematic review. *Aliment Pharmacol Ther.* 2002;16:51–60.
5. Nielsen OH, Rogler G, Hahnloser D, et al. Diagnosis and management of fistulizing Crohn's disease. *Nat Clin Pract Gastroenterol Hepatol.* 2009; 6:92–106.

6. Agrez M, Gu X, Turton J, et al. The alpha v beta 6 integrin induces gelatinase B secretion in colon cancer cells. *Int J Cancer.* 1999;81:90–97.
7. Agrez MV, Bates RC, Mitchell D, et al. Multiplicity of fibronectin-binding alpha V integrin receptors in colorectal cancer. *Br J Cancer.* 1996;73:887–892.
8. Ra H-J, Parks WC. Control of matrix metalloproteinase catalytic activity. *Matrix Biol.* 2007;26:587–596.
9. Orlichenko LS, Radisky DC. Matrix metalloproteinases stimulate epithelial-mesenchymal transition during tumor development. *Clin Exp Metastasis.* 2008;25:593–600.
10. Lin C-Y, Tsai P-H, Kandaswami CC, et al. Matrix metalloproteinase-9 cooperates with transcription factor Snail to induce epithelial-mesenchymal transition. *Cancer Sci.* 2011;102:815–827.
11. Tan TK, Zheng G, Hsu T-T, et al. Macrophage matrix metalloproteinase-9 mediates epithelial-mesenchymal transition in vitro in murine renal tubular cells. *Am J Pathol.* 2010;176:1256–1270.
12. Baugh MD, Perry MJ, Hollander AP, et al. Matrix metalloproteinase levels are elevated in inflammatory bowel disease. *Gastroenterology*. 1999;117:814–822.
13. Kirkegaard T, Hansen A, Bruun E, et al. Expression and localisation of matrix metalloproteinases and their natural inhibitors in fistulae of patients with Crohn's disease. *Gut*. 2004;53:701–709.
14. Naito Y, Yoshikawa T. Role of matrix metalloproteinases in inflammatory bowel disease. *Mol Aspects Med.* 2005;26:379–390.
15. Vandooren J, Van den Steen PE, Opdenakker G. Biochemistry and molecular biology of gelatinase B or matrix metalloproteinase-9 (MMP-9): the next decade. *Crit Rev Biochem Mol Biol.* 2013;48:222–272.
16. Matusiewicz M, Neubauer K, Mierzchala-Pasierb M, et al. Matrix metalloproteinase-9: its interplay with angiogenic factors in inflammatory bowel diseases. *Dis Markers.* 2014;2014:1–8.
17. Manfredi MA, Zurakowski D, Rufo PA, et al. Increased incidence of urinary matrix metalloproteinases as predictors of disease in pediatric patients with inflammatory bowel disease. *Inflamm Bowel Dis.* 2008;14:1091–1096.
18. Kofla-Dłubacz A, Matusiewicz M, Krzesiek E, et al. Metalloproteinase-3 and -9 as novel markers in the evaluation of ulcerative colitis activity in children. *Adv Clin Exp Med.* 2014;23:103–110.
19. Siloşi I, Boldeanu MV, Mogoantă SŞ, et al. Matrix metalloproteinases (MMP-3 and MMP-9) implication in the pathogenesis of inflammatory bowel disease (IBD). *Rom J Morphol Embryol.* 2014;55:1317–1324.
20. de Bruyn M, Machiels K, Vandooren J, et al. Infliximab restores the dysfunctional matrix remodeling protein and growth factor gene expression in patients with inflammatory bowel disease. *Inflamm Bowel Dis.* 2014;20:339–352.
21. de Bruyn M, Arijs I, De Hertogh G, et al. Serum neutrophil gelatinase B-associated lipocalin and matrix Metalloproteinase-9 complex as a Surrogate marker for mucosal healing in patients with Crohn's disease. *J Crohns Colitis*. 2015;9:1079–1087.
22. Castaneda FE, Walia B, Vijay-Kumar M, et al. Targeted deletion of metalloproteinase 9 attenuates experimental colitis in mice: central role of epithelial-derived MMP. *Gastroenterology*. 2005;129:1991–2008.
23. Santana A, Medina C, Paz-Cabrera M-C, et al. Attenuation of dextran sodium sulphate induced colitis in matrix metalloproteinase-9 deficient mice. *World J Gastroenterol.* 2006;12:6464–6472.
24. Liu H, Patel NR, Walter L, et al. Constitutive expression of MMP9 in intestinal epithelium worsens murine acute colitis and is associated with increased levels of proinflammatory cytokine Kc. *Am J Physiol Gastrointest Liver Physiol.* 2013;304:G793–G803.
25. Meier R, Lutz C, Cosín-Roger J, et al. Decreased fibrogenesis after treatment with pirfenidone in a newly developed mouse model of intestinal fibrosis. *Inflamm Bowel Dis.* 2016;22:569–582.
26. Pittet V, Juillerat P, Mottet C, et al. Cohort profile: the Swiss inflammatory bowel disease cohort study (SIBDCS). *Int J Epidemiol.* 2009;38:922–931.
27. Barascuk N, Veidal SS, Larsen L, et al. A novel assay for extracellular matrix remodeling associated with liver fibrosis: an enzyme-linked immunosorbent assay (ELISA) for a MMP-9 proteolytically revealed neo-epitope of type III collagen. *Clin Biochem.* 2010;43:899–904.
28. Genovese F, Barascuk N, Larsen L, et al. Biglycan fragmentation in pathologies associated with extracellular matrix remodeling by matrix metalloproteinases. *Fibrogenesis Tissue Repair.* 2013;6:1–10.
29. Leeming D, He Y, Veidal S, et al. A novel marker for assessment of liver matrix remodeling: an enzyme-linked immunosorbent assay (ELISA) detecting a MMP generated type I collagen neo-epitope (C1M). *Biomarkers*. 2011;16:616–628.
30. Bay-Jensen AC, Leeming DJ, Kleyer A, et al. Ankylosing spondylitis is characterized by an increased turnover of several different metalloproteinase-derived collagen species: a cross-sectional study. *Rheumatol Int.* 2012;32:3565–3572.
31. Veidal SS, Karsdal MA, Vassiliadis E, et al. MMP mediated degradation of type VI collagen is highly associated with liver fibrosis–identification and validation of a novel biochemical marker assay. *PLoS One*. 2011;6:e24753.
32. Marshall DC, Lyman SK, McCauley S, et al. Selective allosteric inhibition of MMP9 is efficacious in preclinical models of ulcerative colitis and colorectal cancer. *PLoS One*. 2015;10:e0127063.
33. Schaefer BC, Schaefer ML, Kappler JW, et al. Observation of antigen-dependent CD8+ T-cell/dendritic cell interactions in vivo. *Cell Immunol.* 2001;214:110–122.
34. Medina C, Videla S, Radomski A, et al. Increased activity and expression of matrix metalloproteinase-9 in a rat model of distal colitis. *Am J Physiol Gastrointest Liver Physiol.* 2003;284:G116–G122.
35. Ellis AJ, Curry VA, Powell EK, et al. The prevention of collagen breakdown in bovine nasal cartilage by TIMP, TIMP-2 and a low molecular weight synthetic inhibitor. *Biochem Biophys Res Commun.* 1994;201:94–101.
36. Bergheim I, Guo L, Davis MA, et al. Critical role of plasminogen activator inhibitor-1 in cholestatic liver injury and fibrosis. *J Pharmacol Exp Ther.* 2006;316:592–600.
37. Maltz, Schwartz. The role of biologic therapy in the treatment of fistulizing Crohn's disease and maintenance of remission of fistulizing disease. *Medscape Gastroenterol.* 2007; November.
38. Fidder HH, Singendonk MMJ, van der Have M, et al. Low rates of adherence for tumor necrosis factor-α inhibitors in Crohn's disease and rheumatoid arthritis: results of a systematic review. *World J Gastroenterol.* 2013;19:4344–4350.
39. Pedersen G, Saermark T, Kirkegaard T, et al. Spontaneous and cytokine induced expression and activity of matrix metalloproteinases in human colonic epithelium. *Clin Exp Immunol.* 2009;155:257–265.
40. Lakatos G, Hritz I, Varga MZ, et al. The impact of matrix metalloproteinases and their tissue inhibitors in inflammatory bowel diseases. *Dig Dis.* 2012;30:289–295.

40a. Sandborn WJ, Bhandari BR, Fogel R, et al. Randomised clinical trial: a phase 1, dose-ranging study of the anti-matrix metalloproteinase-9 monoclonal antibody GS-5745 versus placebo for ulcerative colitis. *Aliment Pharmacol Ther*. 2016;44:157–169.

41. Meijer MJW, Mieremet-Ooms MAC, van der Zon AM, et al. Increased mucosal matrix metalloproteinase-1, -2, -3 and -9 activity in patients with inflammatory bowel disease and the relation with Crohn's disease phenotype. *Dig Liver Dis.* 2007;39:733–739.
42. Efsen E, Saermark T, Hansen A, et al. Ramiprilate inhibits functional matrix metalloproteinase activity in Crohn's disease fistulas. *Basic Clin Pharmacol Toxicol.* 2011;109:208–216.
43. Scharl M, Frei S, Pesch T, et al. Interleukin-13 and transforming growth factor β synergise in the pathogenesis of human intestinal fistulae. *Gut*. 2013;62:63–72.
44. Bay-Jensen AC, Platt A, Byrjalsen I, et al. Effect of tocilizumab combined with methotrexate on circulating biomarkers of synovium, cartilage, and bone in the LITHE study. *Semin Arthritis Rheum.* 2014;43:470–478.
45. Mortensen JH, Godskesen LE, Jensen MD, et al. Fragments of citrullinated and MMP-degraded vimentin and MMP-degraded type III collagen are novel serological biomarkers to differentiate Crohn's disease from ulcerative colitis. *J Crohns Colitis.* 2015;9:863–872.
46. Wiberg C, Hedbom E, Khairullina A, et al. Biglycan and decorin bind close to the n-terminal region of the collagen VI triple helix. *J Biol Chem.* 2001;276:18947–18952.
47. Högemann B, Edel G, Schwarz K, et al. Expression of biglycan, decorin and proteoglycan-100/CSF-1 in normal and fibrotic human liver. *Pathol Res Pract.* 1997;193:747–751.
48. Alexander AC, Irving MH. Accumulation and pepsin solubility of collagens in the bowel of patients with Crohn's disease. *Dis Colon Rectum.* 1990;33:956–962.
49. Rabbani S, Rabbani A, Mohagheghi MA, et al. A novel approach for repairing of intestinal fistula using chitosan hydrogel. *J Biomater Appl.* 2010;24:545–553.
50. Grgic T, Grgic D, Drmic D, et al. Stable gastric pentadecapeptide BPC 157 heals rat colovesical fistula. *Eur J Pharmacol.* 2016. doi: 10.1016/j.ejphar.2016.02.038.

51. Volpe BB, da Santos Duarte AS, Ribeiro TB, et al. Mesenchymal stromal cells from adipose tissue attached to suture material enhance the closure of enterocutaneous fistulas in a rat model. *Cytotherapy*. 2014;16: 1709–1719.
52. Wang X, Zhou Y, Tan R, et al. Mice lacking the matrix metalloproteinase-9 gene reduce renal interstitial fibrosis in obstructive nephropathy. *Am J Physiol Physiol.* 2010;299:F973–F982.
53. Tan TK, Zheng G, Hsu TT, et al. Matrix metalloproteinase-9 of tubular and macrophage origin contributes to the pathogenesis of renal fibrosis via macrophage recruitment through osteopontin cleavage. *Lab Invest.* 2013; 93:434–449.
54. Zheng G, Lyons JG, Tan TK, et al. Disruption of E-cadherin by matrix metalloproteinase directly mediates epithelial-mesenchymal transition downstream of transforming growth factor-beta1 in renal tubular epithelial cells. *Am J Pathol.* 2009;175:580–591.
55. Scharl M, Rogler G. Pathophysiology of fistula formation in Crohn's disease. *World J Gastrointest Pathophysiol.* 2014;5:205–212.
56. Graham MF, Bryson GR, Diegelmann RF. Transforming growth factor beta 1 selectively augments collagen synthesis by human intestinal smooth muscle cells. *Gastroenterology*. 1990;99:447–453.
57. Barnard JA, Beauchamp RD, Coffey RJ, et al. Regulation of intestinal epithelial cell growth by transforming growth factor type beta. *Proc Natl Acad Sci U S A.* 1989;86:1578–1582.
58. Yu Q, Stamenkovic I. Cell surface-localized matrix metalloproteinase-9 proteolytically activates TGF-beta and promotes tumor invasion and angiogenesis. *Genes Dev.* 2000;14:163–176.